

# Duty cycle dependence of a periodically poled LiNbO<sub>3</sub>-based electro-optic Solc filter

Eyal Rabia and Ady Arie

We demonstrate that the performance of a periodically poled LiNbO<sub>3</sub>- (PPLN-) based electro-optic Solc filter is dependent on the duty cycle of the crystal. This may limit the performance of the device for applications such as add-drop filtering and switching, owing to the deterioration of the extinction ratio. It is shown that by adding a retarder to the Solc filter it is possible to improve the extinction ratio; thus the dependence of the filter on the duty cycle can be reduced. Using Jones calculus, we analyzed the effect of a variable retarder that can also be rotated on the extinction ratio. We experimentally observed a 6 dB increase in the extinction ratio when we used a half-wavelength retarder. © 2006 Optical Society of America

OCIS codes: 120.2440, 230.2090, 260.1440.

## 1. Introduction

Periodically poled LiNbO<sub>3</sub> (PPLN) was extensively studied in the past decade for quasi-phase-matched nonlinear interactions.<sup>1</sup> However, the reversal of the ferroelectric domains in this material reverses not only the nonlinear coefficient but also the electro-optic coefficient. The reversal of electro-optic coefficient  $r_{33}$  was used previously for demonstrating optical beam deflection<sup>2</sup> and more recently for electro-optic filtering and equalization of gain.<sup>3</sup> Another class of electro-optic device is based on the reversal of coefficient  $r_{51}$ , which also occurs in PPLN.<sup>4</sup> A variety of PPLN devices, such as an actively Q-switched Nd:YVO<sub>4</sub> laser using an electro-optic PPLN,<sup>5</sup> a polarization controller,<sup>6</sup> and an electro-optic Solc-type wavelength filter in PPLN,<sup>7,8</sup> were shown.

In this paper we concentrate on the Solc filter application of the PPLN based on the electro-optic effect in PPLN. Whereas previously the dependence of PPLN-based Solc filters on temperature, voltage, and laser wavelength was studied,<sup>7,8</sup> the duty cycle (defined as the ratio between the positive domain and the poling period) was assumed to be exactly 50%.<sup>4,6-8</sup> However, in some applications, e.g., when the required poling period for first-order interaction

becomes very small, it may be worthwhile to operate at different duty cycles. Furthermore, from a practical point of view, it is hard to manufacture a device with exactly a 50% duty cycle. Deviations from the exact duty cycle may limit the performance of the device in various applications. Unfortunately, the influence of deviations in duty cycle on the device's performance has not been studied.

In this paper we analyze the influence of the duty cycle, using Jones matrix analysis.<sup>9,10</sup> Whereas a device with a 50% duty cycle can rotate an input linear polarization by 90°, different duty cycles will result in elliptical output polarization. This will limit the extinction ratio in applications such as switching and electro-optic filtering. To mitigate its dependence on the duty cycle, we propose and analyze an improvement to the basic electro-optic Solc filter by addition of a retarder between the crystal and the output polarizer. We provide the theoretical optimum solution for any retardation at any azimuth angle. We experimentally verify the analysis by adding either a  $\pi$  or a  $\pi/2$  constant retardation [half-wave ( $\lambda/2$ ) and quarter-wave ( $\lambda/4$ ) retarders, respectively] at a variable azimuth angle to an electro-optic Solc filter operating near 780 nm.

The theoretical analysis is given in Section 2, followed by an explanation of the experimental setup and presentation of results in Section 3. The results are discussed and summarized in Section 4.

## 2. Theoretical Analysis

A Solc-type filter is a spectral filter that is based on wavelength-selective rotation of polarized light.<sup>7</sup> This

The authors are with the Department of Physical Electronics, School of Electrical Engineering, Tel-Aviv University, Tel-Aviv 69978, Israel. A. Arie's e-mail address is ady@eng.tau.ac.il.

Received 8 December 2004; accepted 15 June 2005.

0003-6935/06/030540-06\$15.00/0

© 2006 Optical Society of America

filter is advantageous in applications that require narrow-bandwidth filters. The folded Solc filter consists of  $\lambda/2$  plates and two crossed polarizers.<sup>9</sup> The plates are arranged alternately at azimuth angle  $\pm\theta$  between the two crossed polarizers. The effect of one period of the crystal is shown in Fig. 1. Assuming that the light is linearly polarized in the  $Y$  direction [Fig. 1(a)], and that the first  $\lambda/2$  plate is at an angle of  $\theta$  with respect to the  $Y$  axis, the light will be rotated to an angle of  $2\theta$  [Fig. 1(b)]. It therefore has an angle of  $3\theta$  with respect to the second  $\lambda/2$  plate [Fig. 1(c)], and thus the output light is polarized at an angle of  $4\theta$  with respect to the  $Y$ -axis [Fig. 1(d)]. Every additional  $\lambda/2$  retarder will further increase the azimuth angle by additional  $2\theta$ . This effect is highly wavelength sensitive, owing to the dispersion of the  $\lambda/2$  plates; hence very narrow optical filters can be obtained.

Owing to the crystal's birefringence, the ferroelectric domains in PPLN can be considered wave plates. For example, a  $\lambda/2$  plate is obtained when the difference between the extraordinary and the ordinary wave vectors satisfies the relation

$$\frac{2\pi n_e}{\lambda} - \frac{2\pi n_o}{\lambda} = \frac{2\pi}{\Lambda}, \quad (1)$$

where  $\Lambda$  is the poling period and  $n_e$  and  $n_o$  are the extraordinary and ordinary refractive indices, respectively. Furthermore, applying an electric field along the  $Y$  axis of the PPLN rotates the index ellipsoid of the crystal, which is equal to rotation of the reversed domains in opposite directions. This enables an electro-optically controlled Solc filter to be achieved.<sup>4</sup>

Previous analysis of the electro-optically controlled Solc filter assumed that the duty cycle is exactly 50%. However, in this paper we extend the theoretical analysis to treat crystals with different duty cycles. We perform this extension by modeling each domain as a Jones matrix.<sup>9–11</sup> The analysis enables us to calculate accurately the dependence of the filter on temperature, wavelength, polarization, number of periods, and applied voltage. The two most important capabilities of Jones calculus are its ability to calculate the field after each period and its ability to perform an exact simulation no matter what the crystal's duty cycle is.

Applying an electric field along the  $Y$  axis of the crystal forms the following matrix<sup>11</sup>:

$$\eta_{\text{pos-neg\_domain}} = \begin{bmatrix} \frac{1}{n_o^2} - r_{22}E_y & 0 & 0 \\ 0 & \frac{1}{n_o^2} + r_{22}E_y & \pm r_{51}E_y \\ 0 & \pm r_{51}E_y & \frac{1}{n_e^2} \end{bmatrix}, \quad (2)$$

where  $r_{51}$  and  $r_{22}$  are the electro-optic coefficients of the PPLN. As the structure inversion is in the  $Z$  axis

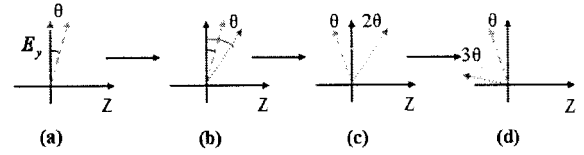


Fig. 1. Rotation of polarization angle in a Solc filter. Dotted curves, the polarization of light; dashed curves, axis of the  $\lambda/2$  plates.

alone, only the elements that relate to the  $Z$  axis change their sign, which means that  $r_{51}E_y$  (for the positive case) becomes  $-r_{51}E_y$  (for the negative case), while the other elements remain the same. Calculation of the eigenvalues and the eigenvectors of square matrix  $\eta_{\text{pos-neg\_domain}}$  gives two new matrices: a  $V$  eigenvector matrix and a  $D$  eigenvalue matrix. The  $V$  matrix defines the rotation matrix from the  $XYZ$  coordinates to the new principal refractive-index ellipsoid coordinates. The  $D$  matrix is a diagonal matrix, which defines the new refractive indices in the new principal axes:

$$D = \begin{bmatrix} \frac{1}{n_x^2} & 0 & 0 \\ 0 & \frac{1}{n_{y'}^2} & 0 \\ 0 & 0 & \frac{1}{n_{z'}^2} \end{bmatrix}, \quad (3)$$

where  $n_{y'}$  and  $n_{z'}$  are the new refractive indices.<sup>11</sup> The elements of the  $D$  matrix define the wave number by the relations

$$k_x = \frac{2\pi n_x}{\lambda}, \quad k_{y'} = \frac{2\pi n_{y'}}{\lambda}, \quad k_{z'} = \frac{2\pi n_{z'}}{\lambda}. \quad (4)$$

The thickness of each domain is  $d_1$  or  $d_2$  (for positive and negative domains, respectively); thus the Jones matrix of a single domain is

$$M_{1,2} = \begin{bmatrix} \exp(ik_x d_{1,2}) & 0 & 0 \\ 0 & \exp(ik_{y'} d_{1,2}) & 0 \\ 0 & 0 & \exp(ik_{z'} d_{1,2}) \end{bmatrix} \quad (5)$$

where  $M_1$  and  $M_2$  are the matrices for the positive and the negative domains, respectively. Knowing these matrices in addition to the fact that  $V_1^{-1} = V_1$ ,  $V_2^{-1} = V_2$  gives<sup>9,10</sup>

$$T_{\text{per}} = V_2^{-1} M_2 V_2 V_1^{-1} M_1 V_1 = V_2 M_2 V_2 V_1 M_1 V_1, \quad (6)$$

where  $T_{\text{per}}$  is the Jones matrix for a single period; therefore the Jones matrix for a crystal with  $N$  periods is

$$T_{\text{cryst}} = T_{\text{per}}^N = (V_2 M_2 V_2 V_1 M_1 V_1)^N. \quad (7)$$

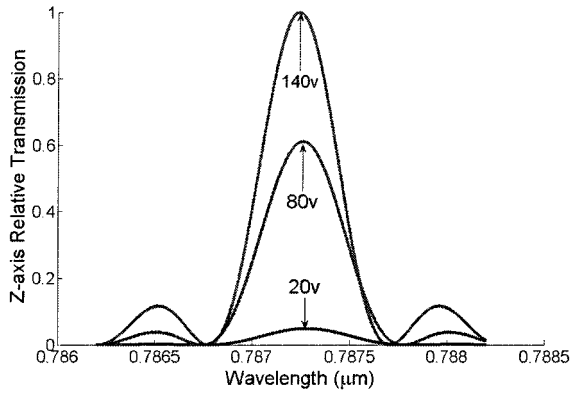


Fig. 2. Transmission along the Z axis as a function of wavelength for three values of the applied voltage. The 1.3 cm PPLN crystal has a period of 10.0  $\mu\text{m}$  and is held at 50  $^{\circ}\text{C}$ .

The light's polarization at the end of the crystal is given by

$$E_{\text{out}} = T_{\text{cryst}} E_{\text{in}}. \quad (8)$$

Figure 2 shows the transmission along the Z axis versus the wavelength for a given temperature for input light polarized along the Y axis. Figure 3 shows the dependence of the transmission on the number of periods for a given voltage.

We demonstrate the influence of the crystal's duty cycle simply by applying different domain lengths ( $d_1 \neq d_2$ ). Figure 4 shows how the Y-axis transmission is affected by the duty cycle. A 50% duty cycle leads to a perfect 90 $^{\circ}$  rotation of the Y-polarized light into linearly polarized light in the Z direction. However, in other duty cycles there is always a residual light that remains in the Y polarization. This will limit the application of the Solc filter in applications that require high extinction ratios (defined here as the ratio between the total power and the residual power in the Y polarization), such as optical switches and add-drop filters.

We propose a way to overcome this critical effect of the duty cycle on the device's extinction ratio by adding a retarder to the device after the crystal output. The Jones matrix that represents the retarder is

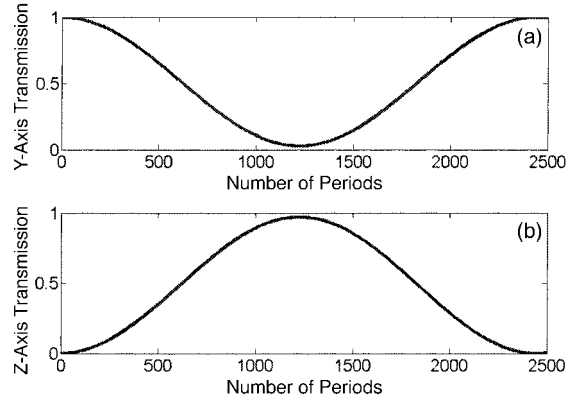


Fig. 3. Transmission at the Solc filter's center wavelength of 787.24 nm along (a) the Y axis and (b) the Z axis as a function of the number of periods. The PPLN crystal has a period of 10.0  $\mu\text{m}$  and is held at 50  $^{\circ}\text{C}$ , and the applied voltage is 140 V.

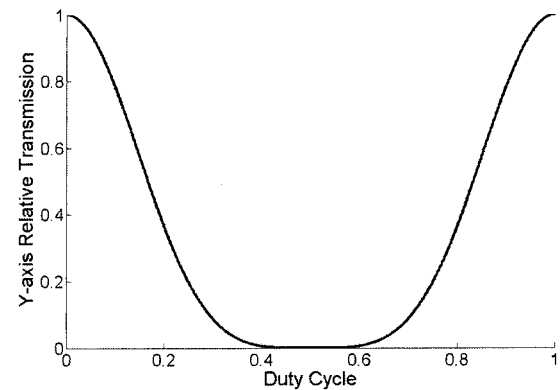


Fig. 4. Transmission at the Solc filter's center wavelength of 787.24 nm along the Y axis as a function of the duty cycle. The 1.3 cm PPLN crystal with a period of 10.0  $\mu\text{m}$  and an applied voltage of 140 V is held at 50  $^{\circ}\text{C}$ .

Figure 5 shows that for any given duty cycle we can find a retarder with a specific azimuth angle [Fig. 5(b)] and a specific retardation [Fig. 5(c)] that leads to a maximal extinction ratio [Fig. 5(a)], which means that using the retarder element helps us to overcome the duty cycle's dependence and to increase the extinction ratio significantly. The best extinction ratio

$$R = \begin{bmatrix} 1 & 0 & 0 & 0 \\ 0 & \cos^2 \psi \exp\left(-i \frac{\Gamma}{2}\right) + \sin^2 \psi \exp\left(i \frac{\Gamma}{2}\right) & -i \sin \frac{\Gamma}{2} \sin 2\psi & 0 \\ 0 & -i \sin \frac{\Gamma}{2} \sin 2\psi & \sin^2 \psi \exp\left(-i \frac{\Gamma}{2}\right) + \cos^2 \psi \exp\left(i \frac{\Gamma}{2}\right) & 0 \end{bmatrix}, \quad (9)$$

where  $\psi$  is the retarder's azimuth angle and  $\Gamma$  is the retardation. The final output field is given by

$$E_{\text{out\_final}} = R E_{\text{out}} = R T_{\text{cryst}} E_{\text{in}}. \quad (10)$$

that was calculated by Jones analysis, with a retarder, is very high ( $\sim 60$  dB), which means that the residual power in the Y axis is negligible. Therefore any slight change in the calculated extinction ratio

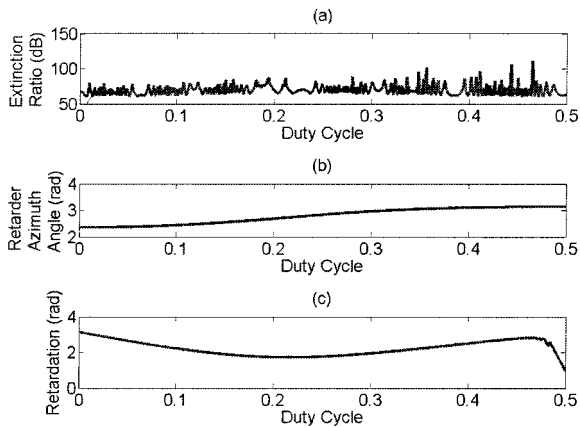


Fig. 5. Calculation of (a) the maximum extinction ratio with the corresponding (b) retarder azimuth angle and (c) retardation. The 1.3 cm PPLN crystal with a period of  $10.0\ \mu\text{m}$  and an applied voltage of 140 V is held at  $50\ ^\circ\text{C}$ . The optical wavelength is the filter's center wavelength of  $787.24\ \text{nm}$ .

causes a significant change in the calculated extinction ratio [Fig. 5(a)]. As it is hard to implement a solution with variable retardation, we repeat the Jones analysis for constant retardation of either  $\pi$  ( $\lambda/2$  plate) or  $\pi/2$  ( $\lambda/4$  plate).

Figures 6(a) and 7(a) show that the  $\lambda/2$  and  $\lambda/4$  plates do not improve the extinction ratio as much as for the full adjustable retarder, but yet it is obvious that a significant improvement is achieved. Figures 6(b) and 7(b) show the required azimuth angles for the  $\lambda/2$  and  $\lambda/4$  plates, respectively. In a  $\lambda/2$  plate the azimuth angle tuning is continuous, whereas in a  $\lambda/4$  plate the optimal angle at duty cycles lower than 0.5 rises continuously until it reaches the value of  $\pi$  at exactly the 0.5 duty cycle. Further increase in the duty cycle requires resetting the retarder angle to  $\pi/2$ , and then it decreases monotonically as the duty cycle increases. Note that at the duty cycle of 0.5 it does not matter whether the  $\lambda/4$  retarder angle is  $\pi$  or  $\pi/2$ , as neither angle alters (nor should alter) the

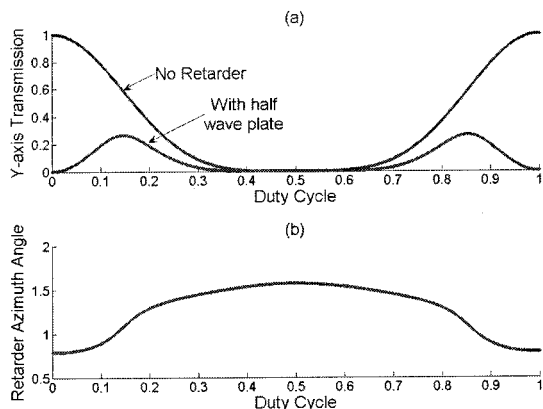


Fig. 6. Transmission at the Solc filter's center wavelength of  $787.24\ \text{nm}$  along the Y axis (a) with and without a  $\lambda/2$  plate retarder and (b) the corresponding retarder's required azimuth angle. The 1.3 cm PPLN crystal with a period of  $10.0\ \mu\text{m}$  and an applied voltage of 140 V is held at  $50\ ^\circ\text{C}$ .

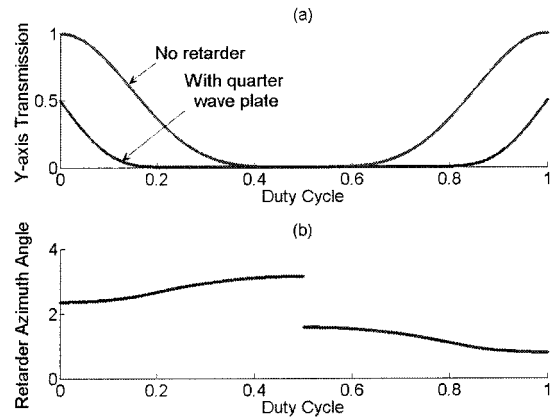


Fig. 7. Transmission at a Solc filter center wavelength of  $787.24\ \text{nm}$  along the Y axis (a) with and without a  $\lambda/4$  plate retarder and (b) the corresponding retarder's required azimuth angle. The 1.3 cm PPLN crystal with a period of  $10.0\ \mu\text{m}$  and an applied voltage of 140 V is held at  $50\ ^\circ\text{C}$ .

polarization of the light coming out of the PPLN crystal.

### 3. Experimental Setup and Results

To test the theoretical prediction we constructed the experimental setup shown in Fig. 8. The light source is a Newport Model 2010M tunable-diode laser operating in the range  $760\text{--}790\ \text{nm}$ . The laser output is already polarized along the Y axis; therefore a polarizer is not needed before the crystal. The laser light is focused into a spot size of  $\approx 84\ \mu\text{m}$  in the middle of the PPLN crystal. The PPLN crystal's dimensions are  $1.3\ \text{cm} \times 1\ \text{mm} \times 1\ \text{mm}$  (XYZ), and the period is  $10\ \mu\text{m}$ ; the duty cycle is 50% with a 5% error range. Two electrodes are sputtered onto the plane perpendicular to the Y axis. A uniform electric field is applied along the Y axis. We heat the crystal to a temperature of  $50\ ^\circ\text{C}$ , which according to the Sellmeier equations<sup>12,13</sup> corresponds to a central wavelength of  $787.24\ \text{nm}$  (center of the Solc filter).

We first measure the Z-axis transmission as function of the laser's wavelength, without the retarder, to observe the wavelength-dependent transmission. Figure 9 shows the theoretical transmission, calculated by Jones analysis, versus the measured transmission at  $50\ ^\circ\text{C}$ . Our measured values exhibit a very close match to the theoretical values. Table 1 compares the important values. In Fig. 9 we have shifted the measured experimental results by  $0.085\ \text{nm}$  to

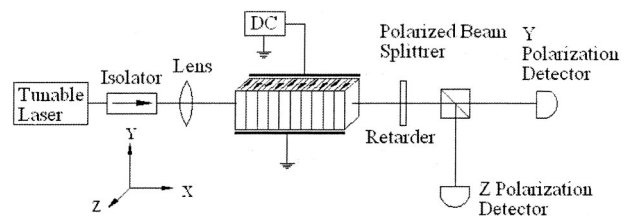


Fig. 8. Experimental setup of a PPLN-based electro-optic Solc filter.

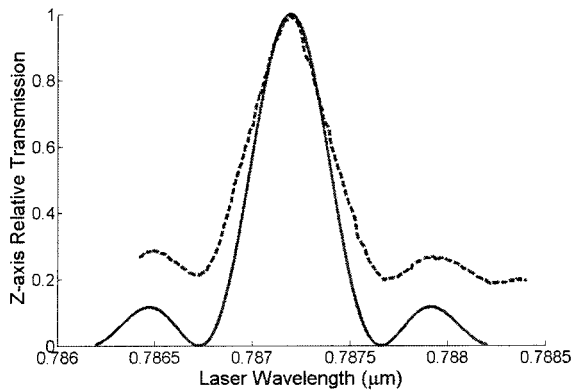


Fig. 9. Transmission along the *Z* axis as a function of wavelength: theoretical (solid curve) versus measured (dotted curve).

Table 1. Comparison of Theoretical Values and Measured Values of the Electro-Optic Solc Filter

Parameter	Theoretical Value	Measured Value
Central wavelength (nm)	787.2	787.285
Filter FWHM (nm)	0.4844	0.4952
Relative transmission	1	0.9918

set the peaks of the theory and the experiment at the same wavelength. The small wavelength difference may be due to inaccuracy in measuring the crystal's temperature or the laser's wavelength or in the finite accuracy of the LiNbO<sub>3</sub> Sellmeier equations.<sup>12,13</sup> The minimum transmission is higher than the theoretical value, owing mainly to residual wavelength-dependent birefringence in the setup as well as to possible deviation from a perfect 50% duty cycle in the PPLN crystal.

In our experiment, the crystal (and thus its duty cycle) is fixed. We assume that it is close to the nominal value of 50% (although we do not know the exact value of the duty cycle), and we concentrate on measuring the effect of adding a retarder on the system's extinction ratio. We add either a  $\lambda/2$  or a  $\lambda/4$  retarder. Figures 10 and 11 show the calculated and

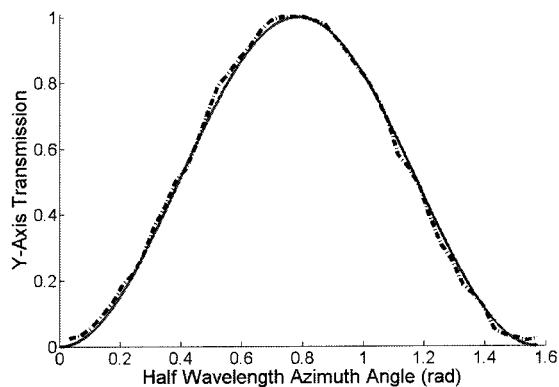


Fig. 10. Calculated (solid curve) and measured (dotted curve) *Y*-axis normalized transmission versus  $\lambda/2$  azimuth angle.

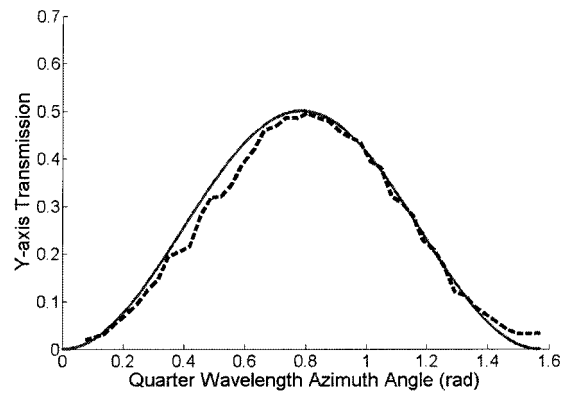


Fig. 11. Calculated (solid curve) and measured (dotted curve) *Y*-axis normalized transmission versus  $\lambda/4$  azimuth angle.

measured *Y*-axis transmission as a function of retarder azimuth angle for  $\lambda/2$  and  $\lambda/4$  retarders, respectively. In the  $\lambda/2$  retarder the linearly polarized light is rotated at two times the azimuth angle<sup>9,10</sup>; hence the entire power level is obtained in the *Y* axis for an azimuth angle of 45°. However, in a  $\lambda/4$  retarder the linear polarization is converted into circular polarization. Hence the maximum transmitted power level with a  $\lambda/4$  retarder is half of that with a  $\lambda/2$  retarder.

We demonstrate good correlation between the measured and the calculated *Y*-axis transmission. It should be noted that keeping a constant retardation and changing the azimuth angle of the retarder provide us with the capability to improve the extinction ratio, no matter what the accurate duty cycle is.

The extinction ratio of the device without any retarder at the center wavelength of the filter is 12.2 dB. When the  $\lambda/2$  plate is added and rotated to minimize the extinction ratio, the ratio is improved to 18.2 dB. Similar improvement is observed with a  $\lambda/4$  retarder. This fourfold improvement shows that by adding a retarder it is possible to compensate for duty cycles that are other than 50%.

#### 4. Conclusions

Jones matrix analysis has enabled us to calculate the performance of a PPLN-based Solc filter. The influence of the PPLN's duty cycle on the device's extinction ratio was studied. It was shown that deviations in the duty cycle strongly affect the performance of the electro-optic Solc filter, and we have suggested a way to overcome this effect by adding a variable retarder with a tunable azimuth angle between the crystal and the output polarizer. We showed theoretically that adding such a retarder can optimize the device's extinction ratio for any given duty cycle by choosing the optimal azimuth angle and retardation.

Implementation restrictions limit us to using constant retardation of  $\lambda/2$  or  $\lambda/4$ . In both cases we have good agreement between the calculations and the measurements of the device's performance when the retarder is used. This correlation shows that one can achieve an improvement of the extinction ratio at any

given duty cycle by using a varying retarder or simply a constant retarder with a variable azimuth angle. The improvement of the extinction ratio opens the possibility for using the electro-optic Solc filter in applications such as optical switching and add-drop filtering.

## References

1. R. L. Byer, "Quasi-phasematched nonlinear interactions and devices," *J. Nonlin. Opt. Phys. Mater.* **6**, 549–592 (1997).
2. M. Yamada and M. Saitoh, "Electric-field induced cylindrical lens, switching and deflection devices composed of the inverted domains in LiNbO<sub>3</sub> crystals," *Appl. Phys. Lett.* **69**, 3659–3661 (1996).
3. A. Arie, A. Burstein, K. Fradkin-Kashi, A. Danielli, and A. Olier, "Dynamic gain equalization based on electro-optic filtering in periodically-poled LiNbO<sub>3</sub>," in *Optical Fiber Communication Conference (OFC)*, Vol. 86 of OSA Trends in Optics and Photonics Series (Optical Society of America, 2003), paper TUM3.
4. Y. Q. Lu, Z. L. Wan, Q. Wang, Y. X. Xi, and N. B. Ming, "Electro-optic effect of periodically poled optical superlattice LiNbO<sub>3</sub> and its applications," *Appl. Phys. Lett.* **77**, 3719–3721 (2000).
5. Y. H. Chen and Y. C. Haung, "Actively Q-switched Nd:YVO<sub>4</sub> laser using an electro-optic periodically poled lithium niobate crystal as a laser Q switch," *Opt. Lett.* **28**, 1460–1462 (2003).
6. J. Shi, X. Chen, Y. Xia, and Y. Chen, "Polarization control by use of the electro-optic effect in periodically poled lithium niobate," *Appl. Opt.* **42**, 5722–5725 (2003).
7. X. Chen, J. Shi, Y. Chen, Y. Zhu, Y. Xia, and Y. Chen, "Electro-optic Solc-type wavelength filter in periodically poled lithium niobate," *Opt. Lett.* **28**, 2115–2117 (2003).
8. Y. M. Zhu, X. F. Chen, J. H. Shi, Y. P. Chen, Y. X. Xia, and Y. L. Chen, "Wide-range tunable wavelength filter in periodically poled lithium niobate," *Opt. Commun.* **228**, 139–143 (2003).
9. A. Yariv and P. Yeh, *Optical Waves in Crystals: Propagation and Control of Laser Radiation* (Wiley, 1984), Chap. 5, pp. 121–152.
10. A. Yariv, *Optical Electronics*, 4th ed. (Holt, Rinehart & Winston, 1991), Chap. 1, pp. 11–29.
11. B. E. A. Saleh and M. C. Teich, *Fundamentals of Photonics* (Wiley, 1991), Subsection 18.2, pp. 713–719.
12. D. H. Jundt, "Temperature-dependent Sellmeier equation for the index of refraction,  $n_e$ , in congruent lithium niobate," *Opt. Lett.* **22**, 1553–1555 (1997).
13. G. J. Edwards and M. Lawrence, "A temperature-dependent dispersion equation for congruently grown lithium niobate," *Opt. Quantum Electron.* **16**, 373–374 (1984).